

Signal Transformation for Effective Multi-Channel Signal Processing

Sunil Kumar Kopparapu^{a,*}

^aTCS Research, Tata Consultancy Services Limited, Mumbai, 400601, Maharashtra, India

ARTICLE INFO

Keywords:

Multi-channel signal Analysis

Signal transformation

Pre-trained models

Audio Embedding

ABSTRACT


Electroencephalography (EEG) is a non-invasive method to record the electrical activity of the brain. The EEG signals are low bandwidth and recorded from multiple electrodes simultaneously in a time synchronized manner. Typical EEG signal processing involves extracting features from all the individual channels separately and then *fusing* these features for downstream applications. In this paper, we propose a signal transformation, using basic signal processing, to combine the individual channels of a low-bandwidth signal, like the EEG into a single-channel high-bandwidth signal, like audio. Further this signal transformation is bi-directional, namely the high-bandwidth single-channel can be transformed to generate the individual low-bandwidth signals without any loss of information. Such a transformation when applied to EEG signals overcomes the need to process multiple signals and allows for a single-channel processing. The advantage of this signal transformation is that it allows the use of pre-trained single-channel pre-trained models, for multi-channel signal processing and analysis. We further show the utility of the signal transformation on publicly available EEG dataset.

1. Introduction

Electroencephalography (EEG) is a method to record the spatial electrical activity of the brain non-intrusively. Typically the instrument used to record EEG has several electrodes mounted on a cap which when placed on the head can sense the electrical activity of the brain at the location or in the spatial vicinity of the electrode. Each electrode captures the brain activity underneath the electrode at a low sampling rate, typically between 250 and 1000 Hz. As a consequence if one uses an EEG instrument with n electrodes, there are n -channels of signals that are simultaneously recorded from each of electrode and are time synchronized. So any analysis on the EEG signal implies processing all the n electrode output signals together to exploit the property that these signal are time synchronized. This, EEG signal, can be considered as an example of a multi-channel signal.


There are several disadvantages and challenges when processing multi-channel signals, like EEG. For example, to mention a few, (a) multi-channel data involves multiple signals recorded simultaneously, which makes it more difficult to identify relevant patterns and interpret results compared to single-channel signals, (b) processing and analyzing multi-channel data requires more computational resources and time longer processing times, (c) different channels may be correlated due to shared sources of brain activity or artifacts, throwing up challenges during analysis, use of techniques to disentangle the signals, (d) interpretation of results from multi-channel EEG can be difficult, relating the observed activity in different channels to specific

*Corresponding author

 sunilkumar.kopparapu@tcs.com (S.K. Kopparapu)

 <http://www.tcs.com> (S.K. Kopparapu)

ORCID(s): 0000-0002-0502527X (S.K. Kopparapu)

 <https://www.linkedin.com/profile/view?id=sunilkopparapu> (S.K. Kopparapu)

arXiv:2412.17478v1 [eess.SP] 23 Dec 2024

Band	Frequency (Hz)	Characteristics
δ	0.5–4	deep sleep and synchronized brain activity
θ	4–8	drowsiness, relaxation, and the early stages of sleep
α	8–12	eyes are closed, relaxation and calmness
σ	12–16	associated with sleep spindles during stage 2 sleep
β	12–30	active thinking, focus, and alertness
γ	30–100	cognitive processing, memory, and perception

Table 1

EEG bands, frequency range, and their characteristics.

cognitive processes or brain regions, (e) lack of standardization in terms of the number of electrodes used to record EEG data or the sampling rate at which the signal is digitized leads to variability in results across studies; making it difficult to compare findings or even build pre-trained foundational models as is common in single-channel signals like audio and speech, (f) a risk of overfitting models to the data, especially if the number of data samples is not sufficiently large relative to the number of channels, leading to poor generalization while analyzing unseen data, and (g) visualizing multi-channel EEG data requires methods to represent both the spatial and temporal aspects in a way that is interpretable. In this paper, we propose a simple yet effective *signal transformation* that overcomes some of these disadvantages of processing and analyzing a multi-channel signal. The proposed transformation allows for representation of a multi-channel signal as a single-channel signal where the transformed signal retains the properties of the original multi-channel signal, making the transformation reversible. The single-channel signal not only allows for better visualization of the signal, but also allows for use of pre-trained foundational models that are available in plenty for single-channel signals, like speech and audio.

The multi-channel EEG signals are low-frequency (low-bandwidth), ranging from 0.1 Hz to about 100 Hz, signals. For the purposes of brain activity analysis, EEG signals are typically divided into different frequency bands, namely, δ , θ , α , σ , β , and γ . These well researched frequency bands have been found to exhibit certain characteristics as shown in Table 1, for example an alert and active brain effects the β band. These frequency bands are essential in EEG signal processing to understand different brain states and activities based on the patterns observed in these frequency ranges. Analyzing and processing multi-channel EEG data often requires specialized knowledge and training in signal processing, and neuroscience.

It is well known, from basics of signal processing literature that signals need to be sampled at twice the maximum frequency present in the signal (also called the Nyquist rate [8]) to preserve the signal characteristics. Since the frequency bands of interest (0.1 to 100 Hz) are low, most EEG instruments sample the brain activities at rates, typically in the range of 250 to 1000 Hz. Observe, in contrast, music, speech and audio signals are sampled at 44.1 kHz for CD quality and typical sampling rates used in speech and audio signal processing is either 8 or 16 kHz. Formally, the Nyquist rate is a fundamental concept in signal processing, which refers to the minimum rate at which a signal must be sampled to accurately represent the signal without losing any information in terms of fidelity. Specifically, the Nyquist rate is twice the highest frequency (bandwidth) of the signal [8]. Our motivation to explore a method for transforming a multi-channel low-bandwidth signal into a single-channel high-bandwidth signal comes from two key observations:

1. **Lack of Pre-trained Models for Low-bandwidth multi-channel EEG:** There are currently no large pre-trained models specifically designed for low-bandwidth EEG signals. This is largely due to the lack of standardization in multi-channel EEG data, which varies both in terms of the number of electrodes used and the sampling rates.

2. Availability of Pre-trained Models for High-bandwidth single-channel Signal: In contrast, there are several well-established pre-trained foundational models, such as VGGish, that are available for high-bandwidth single-channel audio signals. These models can be leveraged for various applications, making them highly useful.

By developing a mechanism to transform a low-bandwidth multi-channel EEG signal into a single-channel high-bandwidth signal, we aim to bridge this gap and potentially enable the use of existing pre-trained models for EEG analysis. Focusing on the question, "Can we use existing pre-trained single-channel (audio or speech) models to analyze or process multi-channel (EEG) signals?", in this paper, we propose a transformation, based on simple signal processing, that allows representing a multi-channel low-bandwidth EEG signal as a single-channel high-bandwidth signal. The proposed transformation is bi-directional (reversible) meaning that the single-channel high-bandwidth signal can be converted back into the original multi-channel low-bandwidth EEG signals without any loss of information. This is the main contribution of the paper. The rest of the paper is organized as follows. We describe the proposed transformation to convert a multi-channel low-bandwidth signal into a single-channel high-bandwidth signal in Section 2, we show in Section 3 the utility of such a transformation by conducting a set of experiments on a publicly available EEG dataset for odour and subject classification. We conclude in Section 4 and provide future directions.

2. Transforming a multi-channel signal to a single-channel signal

Consider a p -channel EEG signal (multi-channel, p electrodes), of duration T (in seconds) sampled at a sampling frequency of f_s Hz. Let $\{e_i[n = 1, \dots, N]\}_{i=1}^p$ denote the p -channel EEG signal where $e_i[n]$ denotes the n^{th} sample in the i^{th} channel and $N = T \times f_s$. The maximum frequency component in $e_i[n]$ is $(f_s/2)$ which is also the bandwidth occupied by each of the individual p -channel's. Note that the cumulative bandwidth of the p -channel EEG signal, if one were to stack the p -channel's one on top of other is $(p \times f_s/2)$, though each individual channel has a bandwidth of $(f_s/2)$. The essential idea of the proposed signal transformation is to *transform* the p -channel EEG signals into a single-channel signal while retaining the individual characteristics of all the p channels of the p -channel EEG signal.

Consider $s[n']$ to be the transformed signal, sampled at a sampling frequency of F_s , namely, the bandwidth of $s[n']$ is $(F_s/2)$. We now describe a process to transform $\{e_i[n : 1, \dots, N]\}_{i=1}^p$, the p -channel EEG signal, each channel having a bandwidth of $(f_s/2)$ into a single-channel $s[n']$ having a bandwidth of $(F_s/2)$, namely,

$$\{e_i\}_{i=1}^p \iff s. \quad (1)$$

Note that the transformation is bi-directional, namely, we are able to reconstruct $\{e_i\}_{i=1}^p$ from s when there is a priori knowledge of how s was obtained from $\{e_i\}_{i=1}^p$. The complete implementation of constructing s from $\{e_i\}_{i=1}^p$ is shown in Algorithm 1. We now describe, in detail, the transformation process based on simple signal processing. There are essentially four steps in the transformation process.

Step #1 For each of the p channels, we compute the well known Fast Fourier Transform (FFT) as shown in Line 9, Algorithm 1, namely,

$$e_i[n] \xrightarrow{FFT} E_i[k] \quad \text{where,} \quad E_i[k] = \sum_{n=0}^{N-1} e_i[n] \exp^{-j \frac{2\pi}{N} kn}, \quad (2)$$

for $k = 0, \dots, (N - 1)$ and has the same number of samples as e_i . Note that the maximum frequency component in E_i is $(f_s/2)$ and the k^{th} sample, $E_i[k]$ corresponds to the amplitude of the frequency component $\left(k \times \left(\frac{f_s/2}{(N-1)}\right)\right)$ Hz in the signal e_i .

Step #2 Now we *stretch* E_i so that the stretched $E_i^{stretch}$ has a maximum frequency of $(F_s/2p)$. This is essentially an index stretching operation, where we take $E_i[k]$ where k runs from $1, \dots, N$ and map those indices to a new set of indices, namely, k' which runs from $1, \dots, \alpha N$, where $\alpha = (F_s/2p)$. As captured in Line 11, Algorithm 1, the frequency domain signal $E_i[k]$ is re-indexed to construct $E_i^{stretch}[k']$, namely,

$$E_i[k] \xrightarrow{k'=\alpha k} E_i^{stretch}[k'] \quad (3)$$

where $\alpha = (F_s/2p)$ and $k = 0, \dots, (N - 1)$. Note that the N samples in E_i would result in αN samples in $E_i^{stretch}$, namely, $k' = 0, \dots, \alpha(N - 1)$. Observe that the value of $E_i^{stretch}[k']$ is the same as the value of the k^{th} sample, $E_i[k]$. However, $E_i^{stretch}[k']$ corresponds to the frequency component $\left(\alpha \times k \times \left(\frac{f_s/2}{(N-1)}\right)\right)$ Hz while $E_i[k]$ corresponds to the frequency component $\left(k \times \left(\frac{f_s/2}{(N-1)}\right)\right)$ Hz. While the maximum frequency component in $E_i[k]$ is $(f_s/2)$, the maximum frequency component in $E_i^{stretch}$ is $(F_s/2p)$. This makes sure that when all the p -channels are stacked together, the combined bandwidth of the p -channel's is $(F_s/2)$. The process of stretching or reindexing from the implementation perspective is best understood with the help of Algorithm 1.

Step #3 We now concatenate or stack the p -channels of $\{E_i^{stretch}[k']\}_{i=1}^p$ on top of one another as shown in Figure 2 to form a single-channel signal of bandwidth $(F_s/2)$. Namely,

$$\{E_i^{stretch}[k']\}_{i=1}^p \xrightarrow{\text{stack}} S[k']. \quad (4)$$

Note that we could stack the p -channels in $p!$ different ways. However, in our implementation, without loss of generality, we choose to stack the p -channels such that the $(i + 1)^{th}$ channel was stacked on top of the i^{th} channel as shown in Figure 2. Line 12 to 21 in Algorithm 1 captures the implementation of the stacking $\{E_i^{stretch}[k']\}_{i=1}^p$ to construct $S[k']$.

Step #4 As the last step in the signal transformation process we compute the inverse FFT (IFFT) of $S[k']$ to construct the time domain signal $s[n']$ (Line 23, Algorithm 1), namely,

$$S[k'] \xrightarrow{IFFT} s[n'] \quad \text{where,} \quad s[n'] = \frac{1}{N} \sum_{k'=1}^N S[k'] \exp^{j\frac{2\pi}{N}k'n'}. \quad (5)$$

Note that the bandwidth of the time domain single-channel signal $s[n']$ is $(F_s/2)$.

Figure 1 shows the i^{th} channel of the EEG signal $e_i[n]$ (top), and its spectral representation $E_i[k]$ (middle) and the stretched version of $E_i[k]$, namely, $E_i^{stretch}[k']$ (bottom). For visual clarity, we use spectrogram of the signals $e_i[n]$ instead of showing the frequency domain signal $E_i[k]$. Figure 2 shows the complete process of constructing a higher bandwidth single-channel signal from low bandwidth multi-channel signals, namely,

$$\underbrace{\{e_i[n]\}_{i=1}^p \xrightarrow{FFT} \{E_i[k]\}_{i=1}^p}_{\text{Step #1}} \xrightarrow{k'=\alpha k} \underbrace{\{E_i^{stretch}[k']\}_{i=1}^p}_{\text{Step #2}} \xrightarrow{\text{stack}} \underbrace{S[k']}_{\text{Step #3}} \xrightarrow{IFFT} \underbrace{s[n']}_{\text{Step #4}}. \quad (6)$$

The implementation of the process of transforming a multi-channel signal into a single-channel signal (6) is captured in Algorithm 1. As mentioned earlier, the transformation process uses fairly well known signal processing techniques and is self-explanatory. However, we would like to mention that

`linspace(0, f_s , N')` (Line 6) is a well known NumPy function that generates N' evenly spaced values between 0 and f_s . The whole process of stacking or reindexing (4) is implemented as shown from Line 12 to 21 which allows to transfer the amplitude associated with the stretched i^{th} (Line 11) channel frequency of the EEG signal to the *closest* frequency available in the desired signal, S obtained using (Line 6) described earlier. It should be noted that by reversing the sequence of operations seen in (6), we can get back $\{e_i[n]\}_{i=1}^p$

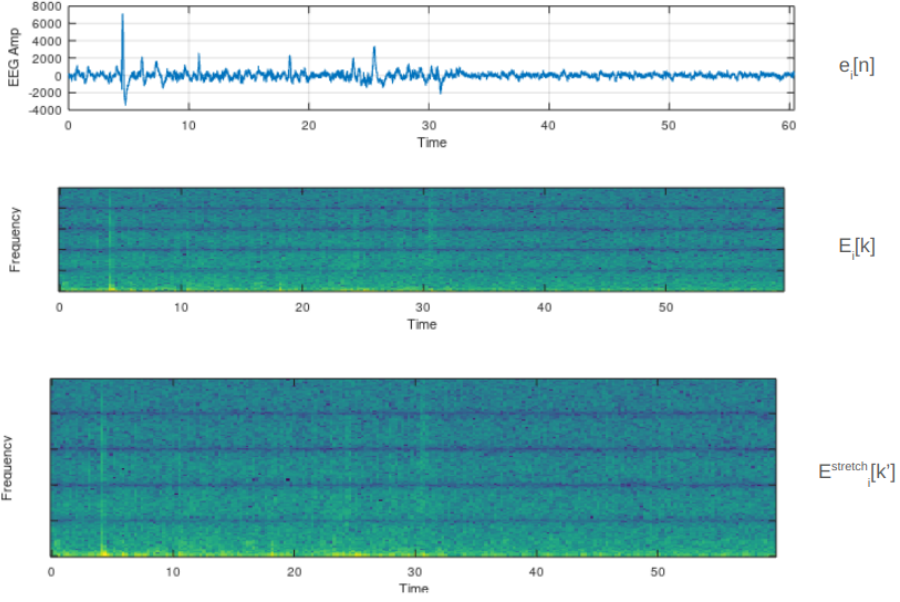


Figure 1: Sample of a single-channel EEG signal of bandwidth $(f_s/2)$ (Top, e_i), spectral representation of e_i (Middle, E_i), and stretched spectral representation with bandwidth $(F_s/2p)$ (Bottom, $E_i^{stretch}$).

from $s[n']$. Namely,

$$s[n'] \xrightarrow{FFT} \underbrace{S[k']}_{(F_s/2)} \xrightarrow{\text{unstack}} \underbrace{\{E_i[k']\}_{i=1}^p}_{(F_s/2p)} \xrightarrow{k=(1/\alpha)k'} \underbrace{\{E_i[k]\}_{i=1}^p}_{(f_s/2)} \xrightarrow{IFFT} \{e_i[n]\}_{i=1}^p \quad (7)$$

Typical values of f_s is around 250 Hz (EEG signal) while typical F_s is 8 or 16 kHz (audio). We hypothesize that $s[n']$ constructed as described in this section represents all the information in the p channel's, namely, $\{e_i[n]\}_{i=1}^p$ in a single-channel signal, namely, $s[n']$. The process of this multi-channel to single-channel transformation allows one to (a) process a single-channel signal $s[n']$ instead of processing all the p -channels $\{e_i[n]\}_{i=1}^p$, (b) make use of any of the known audio processing tools and algorithms, especially when F_s is chosen to be 8 or 16 kHz, and more importantly (c) allows the use of existing pre-trained models trained on single-channel signal.

Fortunately, unlike multi-channel signals, there are quite a few pre-trained models for single-channel signals. For example, VGGish [4] is a popular pre-trained model that has been used for audio classification tasks, YAMNet [11] is another pre-trained deep learning model for sound event detection, DeepSpeech [3] and Wav2Vec [12] are popular pre-trained models used for speech recognition tasks. While almost all of the pre-trained models have not been trained on EEG *like* data, we reckon that they can be used to extract embeddings or features from the transformed signal s which can be treated as features corresponding to all the p channels of EEG, namely, $\{e_i\}_{i=1}^p$.

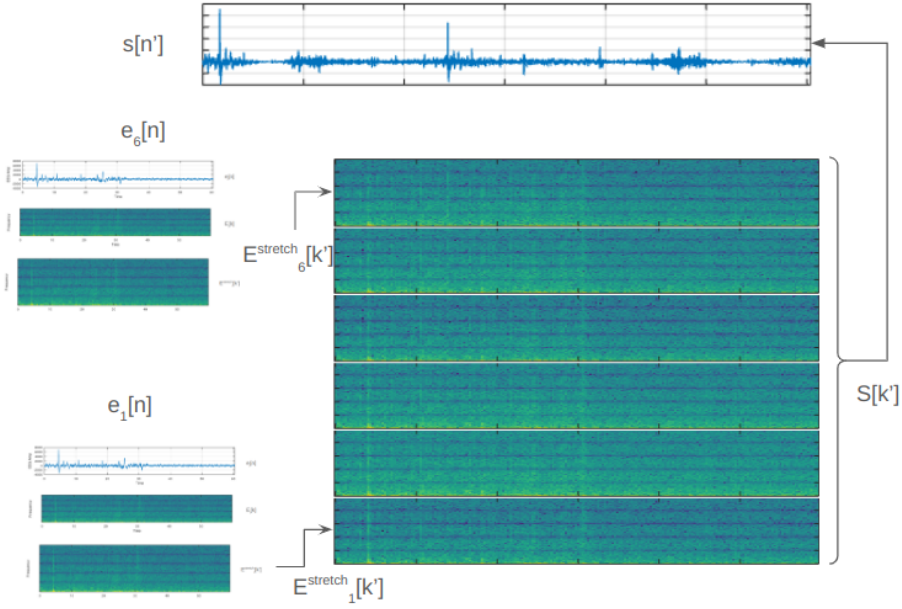


Figure 2: $p = 6$ channel EEG with each channel having a bandwidth of $(f_s/2)$ is stretched to $E_i^{stretch}$ having a bandwidth $((f_s/2) * 6)$ and stacked into a single-channel signal (s) with bandwidth $(F_s/2)$. Implementation details in Algorithm 1.

3. Experimental Analysis

We use the widely used, publicly available odour-EEG dataset (EEGDOT) [7] for training (a) odour-classification [10] system and (b) subject identification [9] system. The EEGDOT dataset consists of a 32 channel EEG signal recorded using the Cerebus system from 11 healthy individuals (8 males and 3 females), right-handed, aged 24.9 ± 3.0 years in response to 13 odour stimuli (rose, caramel, rotten smell, canned peaches, excrement, mint, tea, coffee, rosemary, jasmine, lemon, vanilla, and lavender). Two of the 32 channels are reference channels, making it, $p = 30$ usable channels for analysis. The electrodes for collecting EEG are arranged according to the international 10-20 system, and sampled at $f_s = 1$ kHz. Each sample collected was for a duration of 10 seconds ($N = 10000$ samples), called a trial. In total, EEGDOT dataset has 11 (Subjects) \times 13 (odours) \times 35 (trials) resulting in a total of 5005 30-channel EEG samples. We partition the EEGDOT dataset into non-intersecting 80 : 20 train and test sets. The training set consists of 4004 samples while the remaining 1001 samples were used for test. We retained the split in all our experiments for consistency in experiments.

We converted the 30-channel ($p = 30$) EEG signal into a single-channel high bandwidth audio signal of $F_s = 16$ kHz as described in the previous section following Steps #1, #2, #3, and #4 implemented as mentioned in Algorithm 1. In the first set of experiments, using the single-channel high bandwidth (16 kHz) transformed signal, we extracted the spectrogram (for example, Figure 1 (middle) is the spectrogram of the e_i) using 64 msec (1024 samples) as the window and 48 msec (768 samples) as the overlap. The resulting size of the spectrogram was 513×621 , which is a representation of all the 30 EEG channels *simultaneously*. So each EEG trial was represented by a spectrogram matrix of size 513×621 . We used a Convolutional Neural Network (CNN) architecture [5] as shown in Table 2 for the purpose of odour (13 class, 157945997 trainable parameters) and subject (11 class, 157945739 trainable parameters) classification. The CNN was implemented in *keras* and no hyper parameter tuning was done. As is common, 20% of the train data was

Algorithm 1 Constructing $s[n']$ from $\{e_i[n]\}_{i=1}^p$

```
1: procedure MULTI2SINGLE( $\{e_i[1 : N]\}_{i=1}^p, f_s, F_s$ )  
     $\triangleright f_s$  : sampling rate of  $e_i$ ,  $N$  : number of samples  
     $\triangleright F_s$  : sampling rate of desired signal  $s$   
2:    $t_{sec} = N / f_s$   $\triangleright t_{sec}$  : duration of  $e_i$  in seconds  
3:    $f_{band} = F_s / 2p$   $\triangleright f_{band}$  : bandwidth stretched  $e_i$   
4:    $freq[1 : N] = [0 : N - 1] \times \frac{f_s}{(N-1)}$   $\triangleright$  freq corresponding to  $N$  sample  
5:    $N' = t_{sec} * F_s$   $\triangleright$  Samples in the single-channel  
6:    $F_{desired}[1 : N'] = \text{linspace}(0, F_s, N')$   
7:    $S[1 : N'] = 0; s[1 : N'] = 0$   $\triangleright$  Initialize  
8:   for  $i = 1 : p$  do  
9:      $E_i[1 : N] = \text{FFT}(e_i[1 : N])$   $\triangleright$  Eq (2); Step #1  
10:     $l_f = (i - 1) * f_{band}$ ;  
11:     $f_{stretch}[1 : N] = l_f + \left( freq[1 : N] \times \frac{f_{band}}{f_s} \right)$   $\triangleright$  Eq (3); Stretching.  
12:    for  $j = 1 : N$  do  $\triangleright$  Eq (4); Stacking  
13:       $min_v = 10^{10}; min_1 = -1; min_2 = -1$   
14:      for  $k = 1 : N'$  do  
15:        if  $(|F_{desired}[k] - f_{stretch}[j]| \leq min_v)$  then  
16:           $min_v \leftarrow |F_{desired}[k] - f_{stretch}[j]|$   
17:           $min_1 \leftarrow j; min_2 \leftarrow k$   
18:        end if  
19:      end for  
20:       $S[min_2] = E_i[min_1];$   
21:    end for  
22:  end for  
23:   $s[1 : N'] = \text{IFFT}(S[1 : N'])$   $\triangleright$  Eq (5); Construct  $s$  from  $S$   
24: end procedure
```

used for the purposes of validation. So we had 3203, 801, 1001 samples for training, validation and test respectively with no overlap.

The CNN architecture (Table 2) with a batch size of 32 was run for 150 epochs for odour classification. The training and validation losses (Figure 3a) and accuracy is shown in Figure 3b. The test accuracy for 13 class odour classification was 51.85%. The CNN architecture (Table 2) with a batch size of 32 was run for 25 epochs for subject (11 class) classification. The training and validation losses are shown in Figure 3c while the accuracy is shown in Figure 3d for subject classification. The test accuracy for 11 class subject classification was 99.70%. As seen in Table 3, we achieve the best performance for both odour and subject classification when a single-channel s is used instead of the multi-channel $\{e_i\}_{i=1}^{30}$. Also seen in Table 3 are the performance of SVM (27.63%) and RF (29.85%) classifiers on hand crafted features for odour classification as reported in [10] and subject classification [9]. The total number of features used were 720 which included energy, entropy, discrete wavelet transform for each of the bands.

As mentioned earlier, one of the benefits of transforming a multi-channel EEG signal into a single-channel high bandwidth signal is that it allows the use of existing pre-trained models trained on massive amounts of single-channel data. The use of pre-trained models allows to extract embeddings from these models which

Layer (type)	Output Shape	Param #
spectrogram (Conv2D)	(None, 511, 619, 32)	320
max_pooling2d (MaxPooling2D)	(None, 255, 309, 32)	0
conv2d (Conv2D)	(None, 253, 307, 64)	18496
max_pooling2d (MaxPooling2D)	(None, 126, 153, 64)	0
flatten (Flatten)	(None, 1233792)	0
dense (Dense)	(None, 128)	157925504
[odour] subject (Dense)	(None, [13] 11)	[1677] 1419

Table 2

2D-CNN architecture used for [Odour] and Subject Classification. Using spectrogram features extracted from the transformed single-channel signal s .

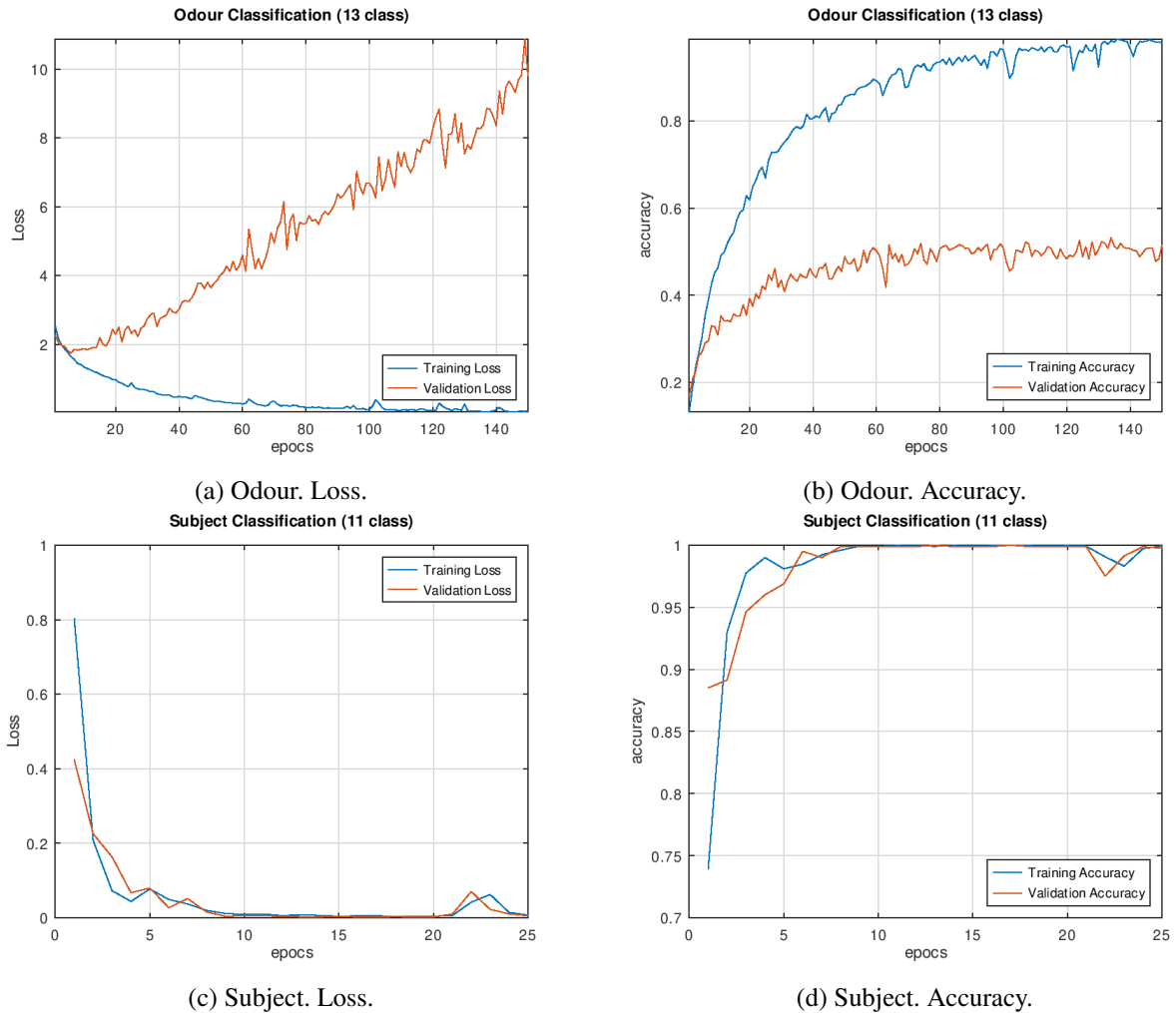


Figure 3: Odour, Subject Classification. Train, Validation plots. For 2D-CNN architecture (Table 2) using spectrogram of the transformed signal as the input features.

can be used as features rather than using handcrafted features for the downstream classification tasks. In the next set of experiments, we used VGGish [1] and YAMNet [2] pre-trained model to extract embeddings, because both of these models have been trained for acoustic or audio event detection. We discounted the use

Signal	Features (size)	Classifier	Odour	Subject
s	Spectrogram (513×621)	2D-CNN	51.85	99.70
$\{e_i\}_{i=1}^{30}$	EEG features (720)	RF	29.85 [10]	97.94 [9]
$\{e_i\}_{i=1}^{30}$	EEG features (720)	SVM	27.63 [10]	93.55 [9]

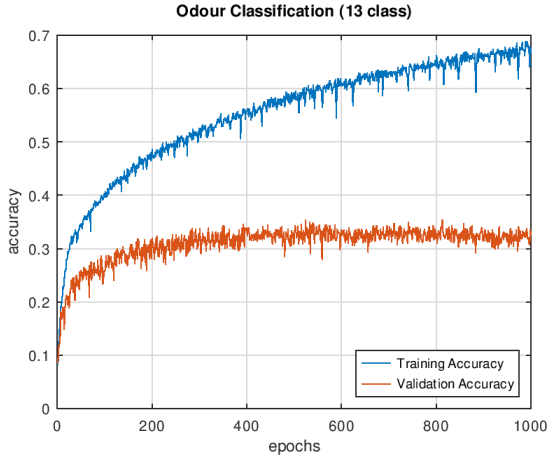
Table 3

Odour and Subject Classification when the transformed single-channel (s) is used versus multi-channel signal ($\{e_i\}_{i=1}^{30}$) for different features and classifiers.

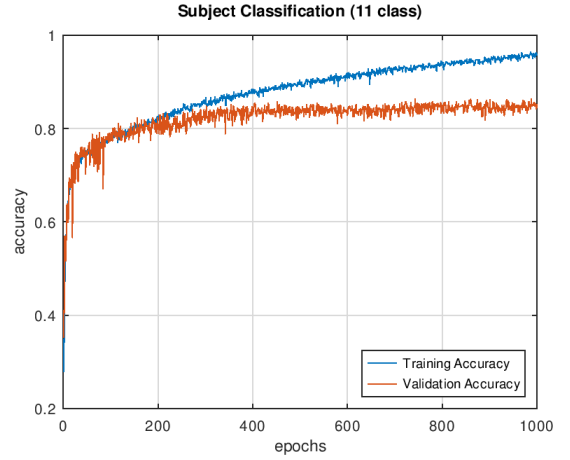
of other pre-trained models like Wav2Vec or DeepSpeech because they are specifically trained for human speech; we feel that the transformed EEG signal is closer to an acoustic event like signal compared to human speech.

The VGGish model gives an embedding of size 128 dimension at 1 Hz. As a consequence, the 10 second 30-channel EEG signal, transformed to a single-channel signal (s), had a representation in the form of a feature vector of size 10×128 . We used a shallow 2D-CNN architecture as shown in Table 4(a). As seen in Table 5 the performance of the odour classification (2066571 trainable parameters) was 30.27% while the performance was 85.91% for subject classification (2066829 trainable parameters). In both the cases, we did not do any hyper-parameter turning and used a batch size of 32 and trained for 1000 epochs. The training and validation accuracy are shown in Figure 4a and Figure 4b for odour and subject classification respectively. Along similar lines, the YAMNet model resulted in an embedding of size 20×521 , where 521 corresponds to the number of audio event classes that YAMNet was trained for. Using a shallow 2D-CNN as mentioned in Table 4(b) we trained for both odour (19097997 trainable parameters) and subject classification (19097739 trainable parameters). As seen in Table 5 the performance of a 2D-CNN architecture using YAMNet embeddings derived from the transformed signal (s) was 33.17% and 94.21% for odour and subject classification respectively. The performance for both odour and subject classification is better when YAMNet pre-trained model is used compared to when VGGish is used; the improvement when YAMNet pre-trained model is used shows a relative improvement of $\approx 9\%$ for both odour $\left(\left(\frac{33.17-30.37}{30.27}\right) \times 100\right)$ and subject $\left(\left(\frac{94.21-85.91}{85.91}\right) \times 100\right)$ classification. However, as seen in Table 5, while the performance, when a pre-trained model is used, is not as good as when the spectrogram features (513×621) of s is used, it nevertheless demonstrates the effective use of existing pre-trained audio models, even though they have not been explicitly trained to process and thereby extracting features low bandwidth multi-channel EEG signals. It should be noted that one of the challenges in processing EEG signals is not only the ability to select as appropriate channel or a set of channels (from the multi-channel signal data) but also the ability to determine the right set of hand-crafted features that best suit the task. Using pre-trained models on the transformed signal s eliminates this challenge. This experimental result demonstrates the effective use of pre-trained models to enable building shallow machine learning models (compare the architecture in Table 2 and Table 4) for odour and subject classification.

For the purpose of comparison, we use the original 30-channel EEG signal to extract spectrogram for each of the 30 EEG channels separately using librosa’s short term Fourier transform, to obtain 30 spectrograms of dimension 62 frequency bins \times 141 time frames, in effect we had a $30 \times 62 \times 141$ tensor representing the EEG signal. We used a 3D-CNN (see Table 6) architecture consisting of 2, convolution followed by average pooling layers followed by Flatten, Dense, BatchNormaization, Dropout(0.5) and Dense layers to train a model for odour and subject classification. We used the default hyper-parameters with a batch size of 32 and 100 epochs. The performance for odour and subject classification was 26.17% and 96.1% respectively (see Table 7). Clearly, deriving spectrogram features from the the transformed single-channel signal (s) performs better (99.70%) than the same spectrogram features derived from the original multi-channel $\{e_i\}_{i=1}^{30}$



(a) Odour Classification.



(b) Subject Classification.

Figure 4: Odour and Subject classification train and validation accuracy plots for 2D-CNN architecture (Table 2(a)) using VGGish embeddings.

Layer (type)	Output Shape	Param #
vggish (Conv2D)	(None, 8, 126, 64)	640
max_pooling2d_2 (MaxPooling2D)	(None, 4, 63, 64)	0
flatten_1 (Flatten)	(None, 16128)	0
dense_1 (Dense)	(None, 128)	2064512
[odour] subject (Dense)	(None, [13] 11)	[1677] 1419

(a) 2D-CNN architecture with VGGish embeddings.

Layer (type)	Output Shape	Param #
yamnet (Conv2D)	(None, 18, 519, 64)	640
max_pooling2d_2 (MaxPooling2D)	(None, 9, 259, 64)	0
flatten_1 (Flatten)	(None, 149184)	0
dense_1 (Dense)	(None, 128)	19095680
[odour] subject (Dense)	(None, [13] 11)	[1677] 1419

(b) 2D-CNN architecture with YAMNet embeddings.

Table 4

Shallow 2D-CNN architecture using (a) VGGish embeddings and (b) YAMNet embeddings derived from the transformed single-channel signal s .

signal (96.10%) for subject classification. Similar enhanced performance is observed for odour classification, compare 51.85% to 26.17% (Table 7). This enhanced performance can be attributed to the proposed signal transformation process that allows the deep learning architecture to *view all the 30-channels together* as a single unit rather than have them viewed as a stack of 30 spectrograms.

To sum up the experimental observations as seen from Table 3, Table 5, and Table 7,

1. The best performance for odour (subject) classification is 51.85% (99.70%) is obtained using the spectrogram features extracted from the single-channel transformed signal (s) using a 2D-CNN architecture. The improved performance compared to any features (spectrogram or handcrafted) extracted from the 30 individual EEG channels (e_i) demonstrates the usefulness of transforming a multi-channel low-bandwidth signal into a single-channel signal.

Signal	Features (size)	Classifier	Odour	Subject
s	Spectrogram (513×621)	2D-CNN	51.85	99.70
s	VGGish (10×128)	2D-CNN	30.37	85.91
s	YAMNet (20×521)	2D-CNN	33.17	94.21
s	VGGish (1280)	RF	38.26	87.01
s	VGGish (1280)	SVM	16.98	68.53
s	YAMNet (10420)	RF	38.66	93.91
s	YAMNet (10420)	SVM	25.77	88.71

Table 5

Odour and Subject Classification using the transformed single-channel signal (s) to demonstrate the use of existing pre-trained single-channel models (VGGish and YAMNet).

Layer (type)	Output Shape	Param #
conv3d (Conv3D)	(None, 28, 60, 139, 32)	896
average_pooling3d (AveragePooling3D)	(None, 14, 30, 69, 32)	0
conv3d_1 (Conv3D)	(None, 12, 28, 67, 64)	55360
average_pooling3d_1 (AveragePooling3D)	(None, 6, 14, 33, 64)	0
conv3d_2 (Conv3D)	(None, 4, 12, 31, 128)	221312
max_pooling3d (MaxPooling3D)	(None, 2, 6, 15, 128)	0
flatten (Flatten)	(None, 23040)	0
dense (Dense)	(None, 512)	11796992
batch_normalization (BatchNormalization)	(None, 512)	2048
dropout (Dropout)	(None, 512)	0
[odour] subject (Dense)	(None, [13] 11)	[6669] 5643

Table 6

3D-CNN Architecture used with $\{e_i\}_{i=1}^{30}$. Total trainable parameters for odour and subject classification is 12083277 and 12082251 respectively.

Signal	Features (size)	Classifier	Odour	Subject
s	Spectrogram (513×621)	2D-CNN	51.85	99.70
$\{e_i\}_{i=1}^{30}$	Spectrogram ($30 \times 62 \times 141$)	3D-CNN	26.17	96.10

Table 7

Odour and Subject Classification using spectrogram derived from the transformed signal s and the original multi-channel signal $\{e_i\}_{i=1}^{30}$.

- While both YAMNet and VGGish are pre-trained models that are used for audio classification tasks, the use of YAMNet embeddings show better performance compared to use of VGGish embeddings across different classifiers for both odour and subject classification tasks (Table 5). While the relative improvement in performance is around 8 – 9% for 2D-CNN and RF classifiers it is much higher (34% for subject and 51% for odour classification) for SVM classifier.
- The performance of both odour and subject classification task using embeddings derived from pre-trained models (VGGish, YAMNet) from the transformed signal (s) is lower compared to the using spectrogram as features extracted from either s or $\{e_i\}_{i=1}^{30}$. This is to be expected because the spectrograms are in some sense a better representation of the signal compared to the embeddings extracted from pre-trained models which have been trained on audio signals that are different from the EEG signals.

4. The best performance using pre-trained models is achieved using YAMNet embeddings + 2D-CNN for subject classification (94.21%) and YAMNet embeddings + RF for odour classification (38.66%) as seen in Table 5.
5. Use of YAMNet or VGGish features demonstrate superior performance (except SVM classifier) compared to extracting hand crafted features from all the 30 EEG channels (Table 3 and 5). This demonstrates that the features extracted as embedding from the single-channel signal (s) using models not specifically trained for EEG signals perform better than even the hand-crafted signal derived from the multi-channel signal (e_i).
6. The difference in performance between odour (best 51.85%) and subject (best 99.70%) classification can be attributed to the EEGDOT data. Fig. 5 shows the t-SNE plot [6] for the training data; better clustered for subject (Fig. 5b) than for odour (Fig. 5a) correlates with the poorer performance for odour classification.

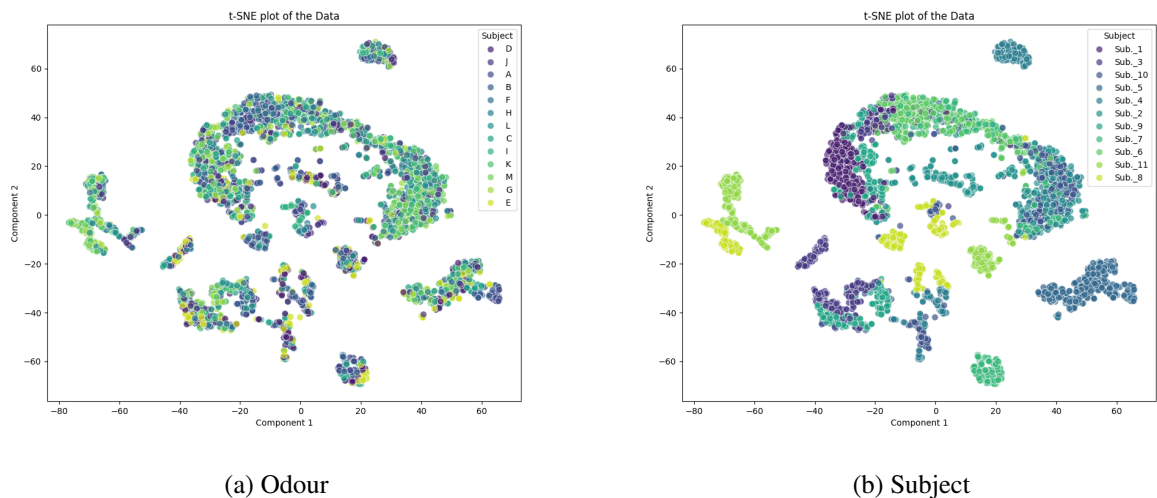


Figure 5: t-SNE plot of the Training data used for (a) odour classification, (b) for subject classification (better clustering).

4. Conclusions

In this paper, we proposed a simple yet effective signal processing method to transform a multi-channel low bandwidth EEG signal into a single-channel high bandwidth signal. The signal transformation is such that it retains all the properties of the original multi-channel signal in the single-channel signal; further the transformation is bi-directional, meaning it allows for reconstructing the multi-channel signal for the single-channel signal. This is the main contribution of this paper. We motivated the need for such a transformation, primarily because the signal transformation allows for a comprehensive, time synchronized view of the multi-channel signal in a single-channel waveform. This is useful, especially in an end-to-end deep learning setup, because there is no extra burden on the end-to-end deep learning setup to *learn the association between different channels* in the multi-channel signal. Single-channel representation derived from the multi-channel signal allows for all the channels to be simultaneously available for processing. Another motivation is that this transformation enables exploit the use of existing pre-trained single-channel acoustic models especially because of the absence of any such pre-trained models for multi-channel signals like EEG. Experimental results show that the single-channel high bandwidth signal is able to retain the properties of the EEG signal

very effectively; indicated by the superior performance for both odour and subject classification compared to hand crafted features extracted from multi-channel EEG signal.

4.1. Discussion

While we have experimented with varying number of convolution layers, different convolution sizes, and varying number of nodes in the dense layers and presented the best performing architectures, we have not experimented with hyper-parameter tuning. There is plenty of scope for further experimentation using different deep learning architectures and hyper-parameter tuning. However, as emphasized earlier, the focus of this paper was on demonstrating that a simple signal processing transformation allowed for a better representation of a multi-channel signal.

The use of pre-trained models trained on acoustic data for acoustic event detection or classification task in the context of EEG data does throw up several questions including the relevance of these pre-trained models for EEG data processing. However, listening to the transformed signal (s) derived from (e_i) made us believe that the transformed signal might have some relevance to acoustic events. The experimental results seem to demonstrate that the pre-trained models are able to extract embeddings that seem to capture the odour and the subject characteristics in the transformed signal. As future work, the single-channel data is neither speech nor audio but converting EEG multi-channel data into a single-channel data, as mentioned in this paper, might allow building models which best work for EEG data.

While both the pre-trained models have been trained for downstream acoustic event detection or classification, it is not clear why one works better than the other. While the focus in this paper was to use the pre-trained models as a black box to extract embeddings or features and not to looking at the architecture or training of the pre-trained models, as future work, it might be a good idea to understand and correlate the performance of odour and subject classification to the architecture and training data associated with the pre-trained model.

References

- [1] Google, 2017. VGGish model checkpoint. https://storage.googleapis.com/audioset/vggish_model.ckpt. Available at: https://storage.googleapis.com/audioset/vggish_model.ckpt.
- [2] Google, 2020.10.06. YAMNet model. <https://www.kaggle.com/models/google/yamnet/tensorFlow2/yamnet/1>. Available at: <https://tfhub.dev/google/yamnet/1>.
- [3] Hannun, A., Case, C., Casper, J., Catanzaro, B., Diamos, G., Elsen, E., Prenger, R., Satheesh, S., Sengupta, S., Coates, A., et al., 2014. Deep speech: Scaling up end-to-end speech recognition. arXiv preprint arXiv:1412.5567.
- [4] Hershey, S., Chaudhuri, S., Ellis, D.P., Gemmeke, J.F., Jansen, A., Moore, R.A., Plakal, M., Platt, D., Saurous, R.A., Seybold, B., et al., 2017. Cnn architectures for large-scale audio classification, in: 2017 IEEE international conference on acoustics, speech and signal processing (ICASSP), IEEE. pp. 131–135.
- [5] LeCun, Y., Bottou, L., Bengio, Y., Haffner, P., 1998. Gradient-based learning applied to document recognition. Proceedings of the IEEE 86, 2278–2324.
- [6] van der Maaten, L., Hinton, G., 2008. Visualizing data using t-sne. Journal of Machine Learning Research 9, 2579–2605.
- [7] Meng, Q.H., Hou, H.R., 2022. Olfactory EEG datasets: EegDot and EegDoc. <https://dx.doi.org/10.21227/59nx-6g46>. doi:10.21227/59nx-6g46.
- [8] Nyquist, H., 1928. Certain topics in telegraph transmission theory. Transactions of the American Institute of Electrical Engineers 47, 617–644.
- [9] Pandharipande, M., Chakraborty, R., Kopparapu, S.K., 2023a. Modeling of olfactory brainwaves for odour independent biometric identification, in: 2023 31st European Signal Processing Conference (EUSIPCO), pp. 1140–1144. doi:10.23919/EUSIPCO58844.2023.10290059.
- [10] Pandharipande, M., Tiwari, U., Chakraborty, R., Kopparapu, S.K., 2023b. Tempo-spectral EEG biomarkers for odour identification, in: 45th Annual International Conference of the IEEE Engineering in Medicine & Biology Society, EMBC 2023, Sydney, Australia, July 24–27, 2023, IEEE. pp. 1–4. URL: <https://doi.org/10.1109/EMBC40787.2023.10340395>, doi:10.1109/EMBC40787.2023.10340395.
- [11] Plakal, M., Ellis, D., 2019. Yamnet: A pretrained deep net for classifying audio events. <https://github.com/tensorflow/models/tree/master/research/audioset/yamnet>.
- [12] Schneider, S., Baevski, A., Collobert, R., Auli, M., 2019. wav2vec: Unsupervised pre-training for speech recognition, in: Proceedings of the 2019 Conference of the North American Chapter of the Association for Computational Linguistics (NAACL), pp. 7–12.